

## Invited talks

# ***Comparing Ptychography, Electron Holography and Phase Plate Techniques for Quantitative Phase Imaging***

Arthur M. Blackburn  
Advanced Microscopy Facility  
Centre for Advanced Materials and Related Technologies (CAMTEC),  
c/o Department of Chemistry  
University of Victoria, Victoria, Canada

Electrons passing through an article under observation in the transmission electron microscope (TEM) are shifted in phase, thus producing observable intensity variations in the image that are dependent upon the phase contrast transfer function of the microscope. In a conventional TEM this contrast is constrained by the lens aberrations, and is spatial frequency dependent, with lower spatial frequencies only giving significant contrast in a defocused condition. This complicates both image interpretation and attempts to quantitatively extract the phase shift arising through certain regions in the sample.

Off-axis electron holography addresses this problem and gives in-focus, low and high-spatial frequency quantitative phase information, which is achieved using a single or multiple electron-prisms. In this arrangement, phase information is most readily gained if one has a structureless reference wave with which to form the interferogram. In practice, though, such a reference wave is not always accessible, which thus limits the applications off-axis electron holography. Consequently, interest continues in inline and reference-wave free methods of reconstructing the phase shift through the sample. One such method is ptychography, which involves computing the exit wave function from a series of convergent diffraction patterns taken from overlapping sample regions [1]. This technique is now more accessible due to advances in the underlying computational algorithms, increasing computational power, fast digital image acquisition systems and improved computer control interfaces available for modern TEMs.

Here examples and comparisons are given between the quantitative phase information gained from electron holograms and ptychographic reconstructions for a range of technologically important samples, discussing the advantages and disadvantages of each method. While these methods allow quantitative phase extraction, phase plates which directly operate on a diffraction plane in the TEM [2], still have a role in allowing rapid identification of low-spatial frequency phase-shift changes in the object with a low electron dose, and further allow rapid estimation of the phase shift in a range of situations.

[1] J.M. Rodenburg, *Advances in Imaging and Electron Physics*, 150, 87-184 (2008).

[2] K. Nagayama, *European Biophysics Journal*, 37, 345-358 (2008).

**Title:**

## **Three-Dimensional Characterization of Shale Porosity**

<sup>1</sup>Patrick M. Price, <sup>1,3</sup>Jatuporn Burns, <sup>1</sup>Kelci Lester, <sup>2</sup>Earl D. Mattson, <sup>2</sup>Hai Huang, and <sup>1</sup>Darryl P. Butt

<sup>1</sup>Boise State University, Department of Materials Science and Engineering

<sup>2</sup>Idaho National Laboratory

<sup>3</sup>Center for Advanced Energy Studies

**Abstract:**

Underground carbon sequestration in oil shale may be a viable strategy to help reduce the impact of carbon dioxide emissions into the earth's atmosphere. Carbon dioxide can be injected into shale reservoirs where it may be sequestered by physical storage of CO<sub>2</sub> in small pores or chemical conversion of the gas to solid minerals such as carbonates. The focus of this study is to investigate the behavior of trapped CO<sub>2</sub> in shale porosity, particularly focusing on interactions with the organic material also known as kerogens. The chemical composition, morphology, pore structure of the Woodford and Eagleford shale are presented here. Three-dimensional characterization of shale using a x-ray tomography, 3D FIB/SEM imaging, and TEM tomography is combined with chemical analysis using energy dispersive x-ray spectroscopy in a SEM. The results of this study, combined with gas transport modeling, will provide insight into fluid and gas storage and transport in these materials.

## Characterization of Radiation Induced Microstructure in UO<sub>2</sub>

Lingfeng He\*, Jian Gan  
Idaho National Laboratory, Idaho Falls, ID 83415  
[Lingfeng.He@inl.gov](mailto:Lingfeng.He@inl.gov),

### Abstract

Uranium dioxide (UO<sub>2</sub>) is the most widely used nuclear fuel in commercial light water reactors. The cumulative radiation damage during the fission process causes severe degradation in the thermophysical properties of UO<sub>2</sub> fuels, which limits their lifetime and increases their operational cost. There are four main sources for decreasing the thermal conductivity during reactor-irradiation: i) irradiation induced defects, ii) solid fission products, iii) fission gas and volatile fission products, and iv) fission gas precipitation and porosity evolution. Therefore, investigating the defect production and evolution, and fission product transport under irradiation, and revealing their physical mechanisms is of great importance in understanding the degradation of thermophysical properties of UO<sub>2</sub> fuels. In this work, *in-situ* transmission electron microscopy (TEM) observation of defect nucleation and evolution under ion irradiation was conducted to understand the radiation damage mechanisms in UO<sub>2</sub>. In addition, irradiation induced microstructure, including dislocation loops, inert gas bubbles, and lunar crater features are characterized using high resolution transmission electron microscopy (HRTEM), scanning transmission electron microscopy (STEM) equipped with electron dispersive X-ray spectroscopy (EDS) and electron energy loss spectroscopy (EELS) as well as atom probe tomography (APT).

## Mapping Plasmons, Structure, and Composition in Complex Bimetallic Nanostructures

Emilie Ringe, Department of Materials Science and NanoEngineering & Department of Chemistry, Rice University, Houston, TX

The catalytic and optical properties of metal nanoparticles can be combined to create platforms for light-driven chemical energy storage and enhanced in-situ reaction monitoring. However, the heavily damped plasmon resonances of many catalytically active metals (e.g., Pt, Pd) prevent this dual functionality in pure nanostructures. The addition of catalytic metals at or close to the surface of efficient plasmonic particles thus presents a unique opportunity *if* the resonances can be conserved after coating.

Here, electron-based techniques (electron-energy loss, cathodoluminescence, and energy dispersive X-ray spectroscopy) are used to characterize two bimetallic systems, Au/Pd octopods (Fig. 1) and Pt-decorated Au prisms (Fig. 2). We show that these Au particles incorporating catalytically active but heavily damped metals sustain multiple size-dependent LSPRs that are strongly localized at the particle tips or edges, depending on the mode energy. Tomography and composition mapping unravels the availability of catalytic metal at the surface of the particle. The formation and alignment of Pt on gold prisms is studied, unraveling the morphology of the 3-5 nm Pt clusters produced. Finally, we discuss the applications of such plasmonic-catalytic bimetallic systems in photo-enhanced catalysis and sensing applications.

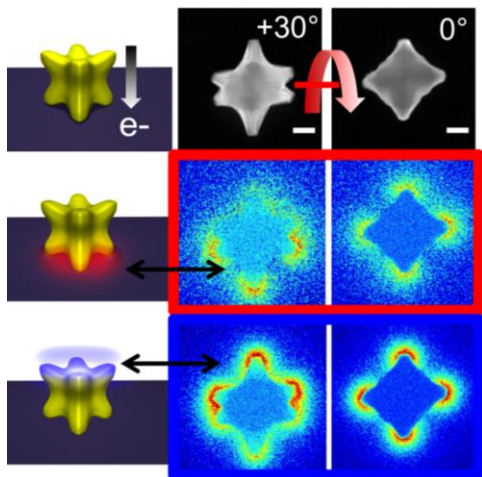
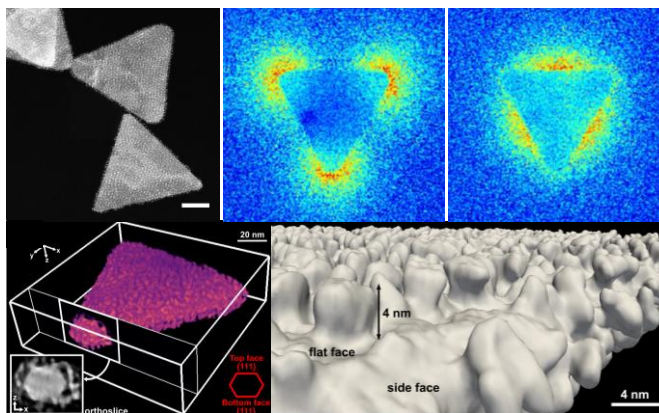


**Figure 1:** Drawings (left), HAADF-STEM (top right) and EELS maps (middle and bottom right) of the localized surface plasmon resonances in Au/Pd octopod nanoparticles.<sup>1,2</sup>

**Figure 2:** HAADF-STEM (top left), plasmon maps (top middle and right) and tomographic reconstructions for Pt-decorated Au nanoprisms.<sup>3</sup>



1. DeSantis, C. J. and S. E. Skrabalak. 2012. Size-Controlled Synthesis of Au/Pd Octopods with High Refractive Index Sensitivity. *Langmuir* 28: 9055-9062
2. Ringe, E., C. J. DeSantis, S. M. Collins, M. Duchamp, R. E. Dunin-Borkowski, S. E. Skrabalak and P. A. Midgley. 2015. Resonances of Nanoparticles with Poor Plasmonic Metal Tips. *Sci. Rep.* 5: 17431
3. Leary, R. K., A. Kumar, P. J. Straney, S. M. Collins, R. E. Dunin-Borkowski, P. A. Midgley, J. E. Millstone, and E. Ringe, *Submitted*

## Application of Electron Microscopy in Semiconductor Memory Industry

Tyler Lenzi and Du Li  
Micron Technology, Inc.

### Abstract:

Electron Microscopy (EM) is a crucial technique to support product development and manufacture in semiconductor memory industry. The applications of EM in our industry are in three aspects, metrology, failure analysis, and materials analysis. With the shrink of process geometry and the use of new materials, we are facing numerous challenges and/or opportunities in the application of EM today. This talk will start with a brief review on the applications of EM in our industry over the last 10 years. Then, we will present an approach how we deal with the challenge by a real life example. Finally, we will identify a few challenges to stimulate the discussions and seek helps in EM professional society.

In-situ materials characterization at high spatial resolution: A journey through liquids, low temperature and beam damage.

*Robert F Klie*

*Department of Physics, University of Illinois – Chicago, Chicago, IL 60607*

The last few years have seen a paradigm change in the way we characterize materials, with unprecedented improvements in both spatial and spectroscopic resolution being realized by aberration-corrected transmission electron microscopes. While spatial and energy resolutions better than 60 pm and 10 meV have been reported, aberration-correction has also enabled a large variety of in-situ experiments at close to atomic resolution. Using this approach, the intercalation of Li-ions into cathode materials, the dynamics of vacancies, and the interactions between gases and nano-particles can now be directly observed, to only mention a few examples. However, the electron probe current densities required for atomic-resolution imaging are often several orders of magnitude higher than the threshold for electron-beam damage, which will prevent us from analyzing the true structure. Therefore, understanding and controlling the effects of the electron beam on the sample materials is emerging as one of the most important areas of current electron microscopy.

In this presentation, I will focus on the atomic-resolution in-situ microscopy of solid-state materials that can withstand high electron-dose rates. I will also explore the effects of radiolysis by examining the mechanism of bubble formation in water encapsulated between two layers of graphene. Here, I will focus on how to control the electron-dose rates and the formation of unwanted radicals in a liquid. Finally, I will demonstrate how we can use the effects of the electron beam to modify the crystal structure of nano-particles to our advantage. More specifically, I will show how performing in-situ aging experiments of battery cathode materials using a high-intensity electron beam can be correlated with ex-situ electro-chemical experiments to explain the mechanism of capacity loss in Li-ion batteries.

## **Multimodal and multiscale optical, electron, X-ray and ion bioimaging to enhance biofuel feedstocks**

**James Evans**, Environmental Molecular Sciences Laboratory, Pacific Northwest National Laboratory, 3335 Innovation Blvd., Richland, WA James.Evans@PNNL.Gov

### **Abstract:**

Increasing volatility in the petroleum market and concern over the long-term availability of fossil fuels has spawned worldwide research into renewable biofuels. However, the widespread adoption of biofuels relies on the continued improvement of its cost competitiveness when compared to diesel and gasoline. Photoautotrophic algae and chemoautotrophic fungi are two types of organisms being utilized for lipid feedstock production with downstream applications for direct conversion to biodiesel. Multimodal and correlative electron, ion, optical and x-ray imaging combined with microfluidic devices that allow experimental control over the local environment provide a unique opportunity to study lipid metabolism from a structural perspective at both the population and single cell levels. Furthermore, integrating such chemical imaging with corresponding 'omics and systems biology analysis can empower holistic understanding of the underlying mechanisms employed by biosystems to identify traits or pathways that can be modified and controlled to yield fully optimized strains and improve the cost competitiveness of biodiesel. In this talk I will highlight preliminary chemical imaging work toward understanding triacylglycerol accumulation in model algae and fungi. I will also describe new dynamic, label-free and in-situ microscopy capabilities being developed at PNNL to fold into our current multimodal platform to enable even more coverage of the complex biological spatiotemporal landscape.

### **Acknowledgement:**

This work was supported by DOE-BER Mesoscale to Molecules Project #66382. Research was performed at Pacific Northwest National Laboratory (PNNL), a multi-program national laboratory operated by Battelle for the U.S. Department of Energy (DOE) under Contract DE-AC05-76RL01830, and at EMSL, a national scientific user facility sponsored by the Department of Energy's Office of Biological and Environmental Research and located at PNNL.

## **ULTRA-HIGH RESOLUTION THREE DIMENSIONAL IMAGING USING 4PI-SMSN THROUGHOUT WHOLE CELLS**

Fang Huang

Weldon School of Biomedical Engineering, Purdue University, West Lafayette, IN, USA

Major advances in biology have been tightly linked with innovations in microscopy. A major hurdle over the last ~100 years is the limited resolution of light microscopy. The advent of single molecule switching nanoscopy (**SMSN**, also known as PALM/STORM/FPALM) has overcome this fundamental limit by improving the resolution of fluorescence microscopy (250-700 nm) by a factor of ten. This method routinely achieves 20-40 nm lateral resolution and 50-80 nm resolution in the axial direction. While the inferior axial resolution largely restricts the biological discoveries to two-dimensional observations, interferometric SMSN (iPALM or 4Pi-SMSN) achieves unprecedented 10 to 20 nm axial resolution by coherently combining single-molecule emissions in a two opposing-objective setup. It allowed, for the first time, the molecular anatomy of focal adhesions to be mapped with nanometer precision. However, the physical principle of 4Pi geometry limits this approach to isolated structures in thin samples because the single molecule interference pattern repeats every 250 nm in depth. While most of biological processes happen deep in the cellular volume, driving ultra-high resolution imaging deeper into the cell will lead to a new wave of biological discoveries.

Here, we present whole-cell 4Pi-SMSN resulting from the confluence of multiple innovations. Our system, for the first time, allowed super-resolution imaging of a ~10  $\mu\text{m}$  thick sample using 4Pi geometry achieving 10-15 nm resolution throughout the depth. This resolution is 20-50 times higher than conventional microscopy with imaging depth improved by 10-40 fold from the state of art technology of interferometric SMSN. It enables ultra-high resolution three-dimensional imaging for vast majority of the subcellular structures. We demonstrate applications in a range of delicate cellular structures including: bacteriophages, ER, mitochondria, nuclear pore complexes, primary cilia, Golgi complex-associated COPI vesicles, and synaptonemal complexes in whole mouse spermatocytes.

## Electron cryomicroscopy and force spectroscopy data suggest anti-pili antibodies may have a direct role in inhibiting diarrheal disease

Magnus Andersson<sup>1</sup>, Narges Mortezaei<sup>1</sup>, Bhupender Singh<sup>1</sup>, Bernt Eric Uhlin<sup>1</sup>, Annette McVeigh<sup>2</sup>, Stephen J. Savarino<sup>2</sup>, Esther Bullitt<sup>3</sup>

<sup>1</sup> Umeå University, <sup>2</sup> Naval Medical Research Center, <sup>3</sup> Boston University School of Medicine

Pathogenic enterotoxigenic *Escherichia coli* (ETEC) are the major bacterial cause of diarrhea in young children in regions with limited resources, and in travelers to countries where ETEC are endemic. Adhesion pili, also called 'fimbriae', are critical virulence factors for ETEC. These pili initiate colonization of the small intestines by binding and providing sustained adhesion to gut epithelial cells. Under force, ETEC pili unwind from their native helical form to an extended linear conformation, thereby sustaining adhesion by reducing the point-of-contact load between the bacterium and the target cell.

We examine structural and biophysical properties of CS20 pili expressed on ETEC, and compare them with those of another ETEC pilus, colonization factor antigen I (CFA/I), and with P-pili from uropathogenic *Escherichia coli*. Variations in pilus structural and biophysical properties correlate with hydrodynamic loads in the preferred environmental niches of infecting bacterial strains: CFA/I pili require the least force to unwind, followed by CS20 pili and then P-pili, which require the highest unwinding force.

Anti-pili antibodies have a *direct* impact on bacterial adhesion: pilus elasticity is reduced upon antibody binding, through inhibition of the pili's natural capacity to unwind and rewind. In the presence of anti-CS20 antibodies, the force required to unwind a single pilus was increased several-fold and the extension length was shortened several-fold. Similar measurements in the presence of anti-CS20 Fab fragments did not show an effect, indicating that bivalent antibody binding is required to reduce pilus elasticity. We expect, therefore, that antibodies provide a 'lock' between turns of the helix, first increasing the force required to unwind the filament, and then obstructing the ability of the pilus to rewind after the layer-to-layer connection has been broken. We propose a model for an *in vivo* mechanism whereby antibody-mediated disruption of the biomechanical properties of CS20 fimbriae impedes sustained adhesion of ETEC to the intestinal mucosal surface. We conclude from our electron microscopy reconstructions, modeling and force spectroscopy data that adaptation of the biophysical properties of pili are critical for successful invasion of target tissue by bacteria and that modulation of these properties by antibodies or other reagents has promise for the disruption or prevention of bacterial infections.

Further elucidation of intestinal antibodies in mechanical disruption of pilus function can provide insights relevant to ETEC vaccine development.

## CT Scans of Single Cells

**Carolyn A. Larabell**

University of California – San Francisco

Soft X-ray tomography (SXT) is similar in concept to the well-established medical diagnostic technique, computed axial tomography (CAT), except SXT is capable of imaging with a spatial resolution of 50 nm or better. With SXT we can examine whole, hydrated cells (between 10-15  $\mu\text{m}$  thick), eliminating the need for time-consuming embedding and sectioning procedures. Cells are imaged using X-ray energies between the K shell absorption edges of carbon (284 eV,  $\lambda=4.4$  nm) and oxygen (543 eV,  $\lambda=2.3$  nm). In this energy range, photons readily penetrate the aqueous environment while encountering significant absorption from carbon- and nitrogen-containing organic material. Consequently organic material absorbs approximately an order of magnitude more strongly than water, producing a quantifiable natural contrast image of cellular structures. SXT, like other tomography modalities, requires recording images from multiple different viewing angles. By collecting images from multiple angles through 360 degrees of rotation, SXT reconstructions yield information at isotropic resolution.

Images are formed using unique optics called zone plates (ZP). An X-ray ZP optic consists of a number of concentric nanostructured metal rings, or zones, formed on a thin X-ray transmissive silicon nitride membrane. The width of the outermost ring determines the spatial resolution of the ZP lens, whereas the thickness of the rings determines the focusing efficiency. In the microscope we utilize, the condenser ZP lens has an overall diameter of 1 cm, 41,667 zones made with approximately 200 nm thick nickel, and a 5 mm central stop. The high-resolution objective ZP lens has a diameter of 63  $\mu\text{m}$  and an outer zone width of 50 nm to assure the entire cell is in focus.

Because SXT is fast (~ 5 min per tomographic data set), we can examine large numbers of cells. Since organic material absorbs approximately an order of magnitude more strongly than water, the high-contrast image of cellular structures is quantifiable. X-ray absorption follows Beer's Law, therefore the absorption of photons is linear and a function of the biochemical composition at each point in the cell. As a result, a linear absorption coefficient (LAC) value of each voxel can be calculated. For example, lipid drops with high concentrations of carbon are more highly absorbing ( $\text{LAC}=0.7 \text{ m}^{-1}$ ) than fluid-filled vesicles ( $\text{LAC}=0.2 \text{ m}^{-1}$ ).

To determine the location of specific molecules with respect to cellular structures, we developed high numerical aperture cryogenic fluorescence tomography (CFT) for correlated imaging studies. This multi-modal approach - imaging the same cell using both CFT and SXT - allows localization of genetically encoded fluorescent molecules directly in the context of a high-resolution 3-D tomographic reconstruction of the cell. This makes it possible to localize molecules tagged with genetically encoded proteins (XFPs, etc.) without having to fix and permeabilize cells, which is required to allow metal particle entry into cells.

## **Structure and dynamics of the tuberculosis ribosome revealed by cryo-EM**

Junjie Zhang, Department of Biochemistry and Biophysics, Texas A&M University

Tuberculosis (TB) is a chronic infectious disease caused by *Mycobacterium tuberculosis* (*Mtb*). It is linked to high morbidity and mortality worldwide. The success of *Mtb* as a pathogen is largely attributable to its ability to persist in host tissues and resist to many antibiotics. In this study, we use *Mtb* ribosomes as a target to understand the mechanism of its persistence and resistance. Specifically, we focus on the species-specific structural features of the *Mtb* ribosomal RNAs (rRNAs), ribosomal proteins (rProteins) and ribosomal factors (rFactors).

By using single particle cryo-electron microscopy (cryo-EM), we have solved the structures of *Mtb* ribosomes to near atomic resolutions, which revealed conformational changes of its unique rRNAs. We have discovered new rProteins along with the binding of a unique rFactor, the ribosomal silencing factor S. We have also seen the antibiotics bound to the *Mtb* ribosomes. These structural data will provide fundamental insights into the molecular events that trigger persistent *Mtb* infection and potentially advance our understanding of *Mtb*'s resistance against antibiotics and the host immune system.

## Strategies for Cryo Correlative Light and Electron Microscopy (cryo-CLEM)

Cheri M Hampton

Emory University School of Medicine, Department of Pediatrics, Division of Infectious Diseases

Our lab has developed strategies for studying various biological systems using the CLEM imaging workflow. CLEM imaging may combine a number of different imaging modalities, e.g. live cell or fixed fluorescent light microscopy (fLM), cryofLM, transmission electron microscopy (TEM) of vitrified sections, cryo-scanning electron microscopy (cryo-SEM), or cryo-electron tomography (cryo-ET). Our preferred workflow uses cryo-fLM of plunge-frozen, vitrified cells correlated with cryo-electron tomography to associate physiology with the three-dimensional (3D) structural context of events. This imaging workflow is of great importance to the cryo-EM field as unobtrusive electron dense-labeling of cell contents has been a challenge. We have developed protocols for imaging labeled versus unlabeled whole cells, locating labeled and expressed proteins within cells, labeled phage attaching to bacteria, and virus attachment to and entry into cells. Care must be taken in designing each experiment to optimize cell adherence to TEM grids and the timing of induction or application of fluorescent tags or probes. Time-course experiments may be accomplished by plunge-freezing the cells at specified intervals following the application of probes, viruses, or phage. Regions of interest are located on the frozen grid using the Leica Cryo CLEM System (Leica Microsystems). These coordinates are then transferrable to the TEM microscope running SerialEM image acquisition software (DN Mastronarde. *Journal of Structural Biology* **152** (2005), p. 36-51). This allows for precise relocalization of the fluorescently-labeled event with the TEM image and cryo electron tomography 3D volume. Thus, the technique of cryo-CLEM is an important link between cell biology and structural biology.

# Polymerization based regulation of a metabolic enzyme: the structure and evolution of CTP synthase filaments

Justin Kollman

Dept. of Biochemistry, University of Washington

## **Abstract:**

The essential, universally conserved metabolic enzyme CTP synthase (CTPS) forms cellular filaments in bacteria and eukaryotes. In bacteria CTPS filaments are catalytically inactive, with polymerization induced by product and reversed by substrate in a form of ultrasensitive feedback inhibition, and filament assembly is required for maintaining nucleotide homeostasis. However, the function and regulatory role of eukaryotic CTPS filaments remain unclear. Here, we show that human CTPS polymerization is induced by substrate and reversed by product, and that polymerization increases catalytic activity, precisely the opposite of the bacterial enzyme. We present cryo-EM structures of *E. coli* and human CTPS filaments, which differ dramatically in overall architecture and in the conformation of the CTPS protomer. The structures elucidate mechanisms of assembly and enzyme regulation, and reveal for the first time the active conformation of CTPS. We demonstrate a universally conserved substrate and product dependent conformational equilibrium, with CTPS locked in an inactive conformation in the *E. coli* filament and an active conformation in the human filament. This may provide a general mechanism for increasing human CTPS activity in response to metabolic state. Complex allosteric regulation of CTPS polymerization by ligands likely represents a fundamental mechanism underlying polymerization of the large number of other metabolic enzyme filaments.

## Compressive Sensing in Microscopy: a (P)review

Andrew Stevens(1,2), Hao Yang(3), Libor Kovarik(1), Xin Yuan(4), Quentin Ramasse(5), Patricia Abellan(5), Yunchen Pu(2), Lawrence Carin(2), and Nigel D. Browning(1)

1. Pacific Northwest National Laboratory, Richland USA
2. Duke University, ECE, Durham USA
3. Lawrence Berkeley National Laboratory, Berkeley USA
4. Bell Laboratories, Murray Hill USA
5. SuperSTEM, STFC Daresbury Laboratories, Warrington UK

Currently many types of microscopy are limited, in terms of spatial and temporal resolution, by hardware (e.g., camera framerate, data transfer rate, data storage capacity). The obvious approach to solve the resolution problem is to develop better hardware. An alternative solution, which additionally benefits from improved hardware, is to apply compressive sensing (CS) [1]. CS approaches have been shown to reduce dose by as much as 90% in electron microscopy [2, 3, 4]. Optical imaging and microscopy have also seen substantial benefits [5, 6, 7, 8, 9, 10, 11, 12, 13].

This tutorial will briefly introduce the principles of CS. Primarily, we will focus on the setup and modifications necessary for applying CS to a few different types of microscopy and spectroscopy

- Scanning microscopy (e.g., STEM [2], SEM, STXM)
- EELS, EDS, Mass spec
- TEM-video [3], optical-video [7]
- Phase-contrast imaging
- Tomography.

We will show results for a few of these compressive sensing approaches. Moreover, an approach for detecting CS reconstruction errors (i.e., errors introduced by the image processing algorithm) will be discussed.

### References:

- [1] RG Baraniuk. IEEE signal processing magazine 24(4).
- [2] A Stevens, H Yang, L Carin et al. Microscopy 63(1), (2014), pp. 41.
- [3] A Stevens, L Kovarik, P Abellan et al. Advanced Structural and Chemical Imaging 1(1), (2015), pp. 1.
- [4] A Stevens, L Kovarik, P Abellan et al. Microscopy and Microanalysis 21(S3), (2015), pp. 1583.
- [5] M Zhou, H Chen, J Paisley et al. Image Processing, IEEE Transactions on 21(1), (2012), pp. 130.
- [6] Z Xing, M Zhou, A Castrodad et al. SIAM Journal on Imaging Sciences 5(1), (2012), pp. 33.
- [7] X Yuan and S Pang. Biomedical Optics Express 7(3), (2016), pp. 746.
- [8] Y Pu, X Yuan and L Carin. arXiv:14126039.
- [9] Y Pu, X Yuan, A Stevens et al. In AISTATS 2016.
- [10] P Llull, X Liao, X Yuan et al. Optics Express 21(9), (2013), pp. 10526.
- [11] X Yuan, J Yang, P Llull et al. In ICIP 2013 (IEEE).
- [12] J Yang, X Yuan, X Liao et al. Image Processing, IEEE Transactions on 23(11), (2014), pp. 4863.
- [13] X Yuan, P Llull, X Liao et al. In CVPR 2014 (IEEE).

# Nanobeam diffraction scanning in transmission electron microscopes

E.F. Rauch

Univ. Grenoble Alpes, CNRS, SIMAP, F-38000 Grenoble, France

There is a growing interest for nanobeam diffraction mapping technics that allows the characterization of the structure of materials at nanoscale. Basically, in this technique, full series of diffraction patterns are collected in a transmission electron microscope and stored while the focused beam is scanning the sample [1]. One of the main advantage is that the acquired data are available for off-line processing so that essential properties like the local crystallographic texture or the phase distribution may be mapped with a limited beam time.

Diffraction scanning techniques benefit from precession electron diffraction (PED). This is because precession is known to increase the number of reflections and to decrease the dynamic effect on the Bragg reflection intensities, which, in turn, improve the quality of the diffraction patterns. Typically, orientation and phase identifications are greatly improved.

Several post-processing strategies will be presented. This include the now standard template matching approach that has proved to be efficient for orientation and phase identification (Fig.1). Besides, it will be shown that specific structural entities may be highlighted by producing so-called virtual dark-field images [2] and the newly developed construction of electron diffraction correlation coefficient maps that has been shown to retrieve 3D information [3] will be introduced.

[1] E.F. Rauch, M. Véron, Mater. Charact. **98** (2014) 1–9.

[2] E. F. Rauch and M. Véron, Eur. Phys. J. Appl. Phys. (2014) **66**: 10701

[3] Á.K. Kiss, E.F. Rauch, J.L. Lábár, Ultramicroscopy **163** (2016) 31–37.

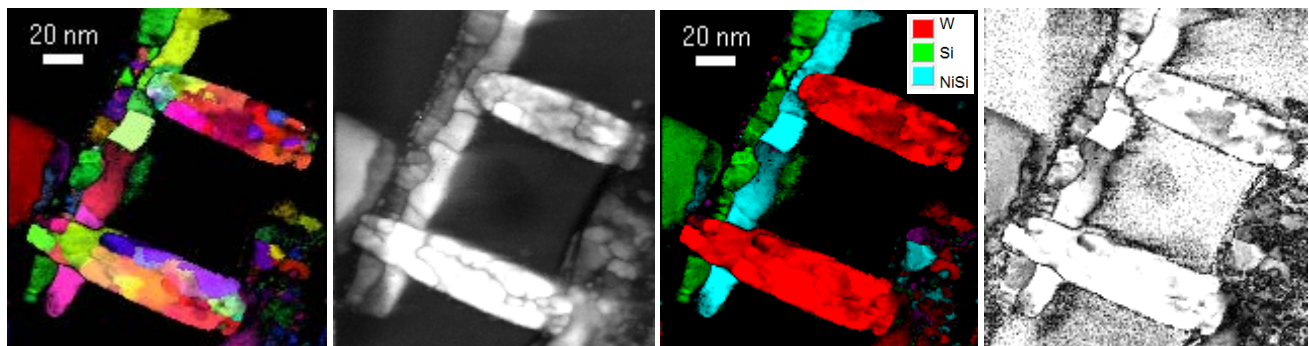


Figure 1: Characterization of an microelectronic device with, respectively, an Crystallographic orientation map, an Index map, a Phase map and a Phase reliability map.

# Applications of Bicrystallography

Peter Moeck, Department of Physics, Portland State University, Portland, OR 97207-0751

The application of bicrystallography [1-3] makes structural units and dislocations superfluous as descriptors of grain boundaries. All there is around an *ideal* (un-relaxed) coincidence site lattice (CSL) grain boundary are predictable atomic positions with certain black-white symmetries. Free energy minimization driven relaxations of such a hypothetical grain boundary structure may lead to the breaking of some or all of the black-white symmetries, just as monochrome space group symmetries may be broken by defects locally in the two real single crystals that make up the bicrystal. Any relaxed (*real*) atomic position will, however, be very close to the predicted un-relaxed (ideal) atomic position as long as that position remains occupied. Grain boundary structures with nine degrees of freedom as predicted by bicrystallography in three dimensions (3D) are, therefore, ideal as atomic level starting structures for free energy minimization calculations. Bicrystallography in two dimensions (2D) allows for straightforward visualizations of edge-on projections of CSL tilt boundaries [3].

A range of CSL [001] tilt boundaries in  $\text{CeO}_2$  were imaged with an aberration corrected Z-contrast Scanning Transmission Electron Microscope (Z-STEM) and striking visual similarities of their (projected) structural units to those of (analogous orientation relationship) grain boundaries in face-center cubic metals, yttria-stabilized zirconia, and  $\text{SrTiO}_3$  were noted in ref. [4]. There is, however, arbitrariness in the choosing of structural units, despite their emergence in connection with free energy minimization calculation and their identification as cores of grain boundary dislocations. The predictive power of structural units is, accordingly, limited to series of grain boundaries in the same material when only one of the five macroscopic degrees of freedom is varied [4]. Our bicrystallography analysis, on the other hand, shows that these structural similarities are simply byproducts of the edge-on projection of the black-white layer groups of the bicrystals in these materials [3]. In short, whenever Bärnighausen trees [5] reveal structural relations (i.e. similarities) between the space groups of different materials, there will (per bicrystallography) also be predictable structural similarities in their analogous orientation relationship grain boundaries.

The 3D atomistic structures of general *ideal* (un-relaxed) grain and phase boundaries cannot be described by CSL orientation relationships, but become predictable by the adaptation [6] of ideas and techniques that were originally developed for the study of quasicrystals. Quasi-bicrystallography in 2D allows again for straightforward visualizations of edge-on projections of general grain boundaries.

Modern ways of visualizing grain boundary structures involve 3D printing. In order to create a 3D printed model, one has to come up with a 3D printable file that one may send off to a professional print shop. A range of proprietary computer aided design programs can be utilized for the creation of such a file. There are also the freeware programs Cif2VRML [7] and Mercury 3.6 from the Cambridge Crystallographic Data Centre [8]) that read atomic coordinates of grain boundary structures (or molecules) in the very well documented Crystallographic Information File (CIF) format [9] and convert them directly into a range of 3D print file formats.

In order to provide a concise structure description in the corresponding grain boundary CIFs, the bicrystal layer group symmetry of a CSL grain boundary stands in for the space group symmetry of the component crystals and the CSL parameters stand in for these crystals' unit cell parameters. In the CIFs that encode the structure of the highest symmetric grain boundary models, only one eighth of the atoms that make up the 3D printed models (i.e. the content of the "asymmetric black-white unit" of the CSL unit cell) need then be included explicitly.

[1] R. C. Pond and W. Bollmann, *Proc. Royal Soc. London A* **292** (1979) 449

[2] R. C. Pond and D. S. Vlachavas, *Proc. Royal Soc. London A* **386** (1983) 95

[3] P. Moeck et al., *Cryst. Res. Technol.* **49** (2014) 708

[4] W. Tong et al., *Acta Mater.* **61** (2013) 3392

[5] U. Müller, *Symmetry Relations between Crystal Structures*, Oxford University Press, 2013

[6] D. Romeu et al., *Phys. Rev. B* **59** (1999) 5134

[7] W. Kaminsky et al., *Powder Diffraction* **29** (2014) S42, freely downloadable at <http://cad4.cpac.washington.edu/Cif2VRMLHome/Cif2VRML.htm>

[8] <http://www.ccdc.cam.ac.uk/Community/blog/post-53/>

[9] <http://www.iucr.org/resources/cif>

## Atom probe tomography of fuels

Assel Aitkaliyeva<sup>1</sup>, Cynthia Papesch<sup>1</sup>, Yaqiao Wu<sup>2</sup>, Haiming Wen<sup>3</sup>

<sup>1</sup>*Idaho National Laboratory, PO Box 1625 MS 6188, Idaho Falls, ID 83415, USA*  
[assel.aitkaliyeva@inl.gov](mailto:assel.aitkaliyeva@inl.gov)

<sup>2</sup>*Department of Materials Science and Engineering, Boise State University, Boise, ID 83725, USA*

<sup>3</sup>*University of Idaho, Moscow, ID 83844, USA*

Dramatic advances in materials characterization capabilities over the last few years enabled the transition of electron tomography (ET) and atom probe tomography (APT) techniques to a much broader research field and their implementation in the characterization of nuclear fuels and highly radioactive materials. Nanoscale characterization has been widely developed for non-nuclear applications, yet in the nuclear arena, particularly for fuels, these modern characterization techniques have not been applied in concert to elucidate fundamental material behavior in metal fuel.

The combination of electron tomography via TEM and APT techniques enables comprehensive 3D analysis of the samples, which is of particular importance for irradiated nuclear fuels and materials because it will provide unprecedented understanding of the nuclear materials systems in 3D at the nanoscale. This has significance as fuel performance codes may use simplistic material property parameters or employ a numerically generated set of microstructures that may not accurately represent statistically meaningful distributions of phase morphology, phase distribution, and local species concentrations.

This study investigated the interdiffusion between U-Pu-Zr metal fuel and cladding via diffusion couple technique, formation of various intermetallic phases and precipitates upon exposure to high temperatures, and fuel-cladding microstructural development at the atomic scale using ET in transmission electron microscope (TEM) and APT technique in localized electrode atom probe (LEAP) instrument.

In addition to fresh transuranic fuels, neutron irradiated U-Mo fuel has been examined using combination of these techniques. It allowed comprehensive atomic-scale characterization of chemical composition of fission gas bubbles formed in U-Mo dispersion fuel—a task that has not been accomplished since the development of this dispersion fuel and discovery of bubble superlattice.

# Nanoscale Chemical Imaging by Photo-induced Force Microscopy

Sung Park

Molecular Vista, 6840 Via Del Oro, Suite 110, San Jose CA 95119, USA

sung@molecularvista.com

Correlating spatial chemical information with the morphology of multi-component nanostructures remains a challenge for the scientific community as many such systems are not easily interrogated in real-space via existing instruments based on optics or electrons. A novel scanned probe technique called Photo-induced Force Microscopy (PiFM) measures the photo-induced polarizability of the sample directly in the near-field by detecting the time-integrated force between the tip and the sample. Imaging with infrared wavelengths specific to different organic components, PiFM can resolve the nanometer-scale distribution of each chemical species in diverse multi-phase and multi-component systems.

When coupled with a widely tunable infrared quantum cascade laser system, a powerful imaging mode, which we call hyPIR (derived from hyperspectral PiFM infrared), can be realized. A hyPIR image consists of a PiFM spectrum (which correlates well with bulk FTIR spectrum for most species) at each pixel of a  $(n \times n)$  image, similar to a confocal micro Raman image, except with  $\sim 10$  nm spatial resolution. By detecting the molecular infrared absorption via mechanical force measurement, PiFM achieves spatial resolution that surpasses the diffraction limit by an astonishing factor of  $\sim 1000\times$ . **Fig. 1** is an example of a hyPIR image where  $128 \times 128$  pixels of PiFM spectrum over  $1400$  to  $1800$   $\text{cm}^{-1}$  range was acquired in 54 minutes. The power and utility of PiFM and hyPIR imaging will be demonstrated by presenting results on several multi-component nano-systems.

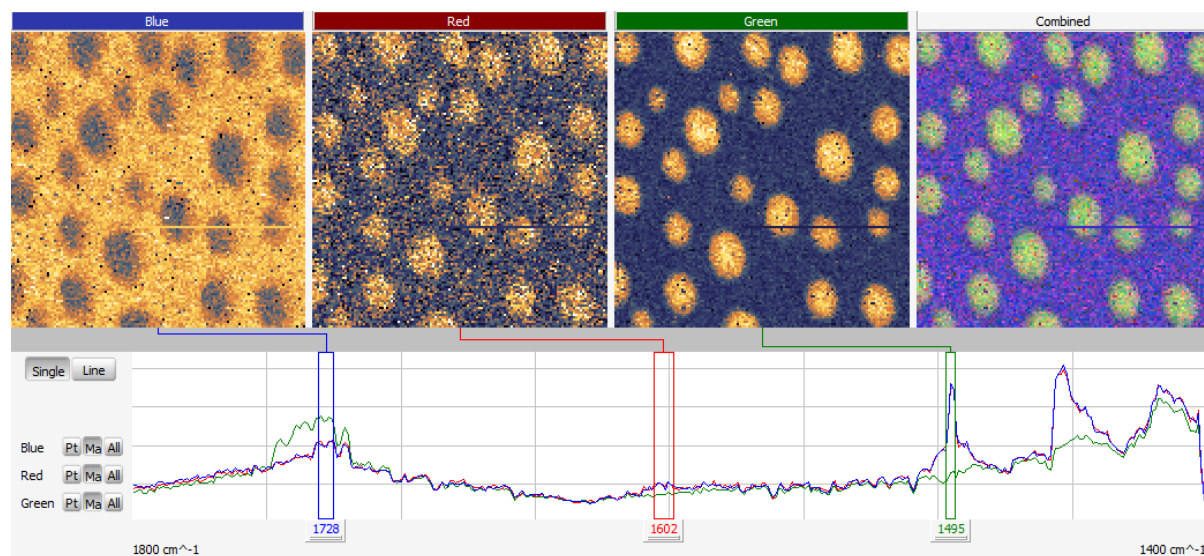


**Fig. 1:** A hyPIR image ( $128 \times 128$  pixels of PiFM spectrum over  $1400$  to  $1800$   $\text{cm}^{-1}$ ) of 5 nm of polystyrene (PS) homopolymer that is spin-coated onto a 2 nm thick poly(methyl methacrylate) (PMMA) homopolymer on top of silicon substrate. Due to the thin PS layer and its immiscibility with PMMA, PS has dewetted into nanoscale droplets. The green, blue, and red spectra are spectra averaged over the background, one circular feature, and another circular feature respectively. Up to three spectral slices (blue, red, and green channels) can be selected to display their intensity maps. Note that even a small difference in spectra leads to clear chemical map (see the red channel at  $1605$   $\text{cm}^{-1}$ ). This  $2 \mu\text{m} \times 2 \mu\text{m}$  hyPIR image took 54 minutes to acquire (each PiFM spectrum over  $1400$  to  $1800$   $\text{cm}^{-1}$  took about 0.2 seconds).

# Image Simulations of Complex Oxides – A guide to better experiments.

Thomas Vogt

University of South Carolina

High Angle Annular Dark Field Scanning Transmission Electron Microscope (HAADF/STEM) and annular bright-field imaging (ABF) are imaging techniques that come close to being *the ultimate nano-imaging tool*. In an HAADF detector mainly incoherent scattering is collected, which from a specimen with appropriate thicknesses is a monotonic function without contrast reversal which greatly simplifies the interpretation of the resulting images. Our work on the Mitsubishi oxidation catalyst based on Mo-V-Te-oxides reveals that active sites of immensely complex oxides and oxide mixtures can be imaged using aberration-corrected STEM and result in transformative advancements in the study of heterogeneous catalysts by using in-situ electron microscopy, including more recently studies at high temperatures.

However, for complex materials and the elucidation of subtle structural details one needs to validate the contrast interpretations using multi-slice or Bloch wave image simulations. Using GPU parallel computing and a “frozen-phonon image simulation” program that allows the simulation of images *with unprecedented structural and compositional complexity* we can now guide our observations in more complex materials. Such computations were unthinkable a decade ago and have only recently been possible to game-changing capabilities provided by GPU chips and large national parallel computing facilities. Recent work set out to compare the structural model of a highly complex low-symmetry ionic conductor based on high-resolution x-ray and neutron scattering with direct imaging using both bright and dark field imaging. The anticipated growth of STEM in materials science mandates that we push and explore boundaries while establishing best practices.

# *in situ* Investigations of Organic Inorganic Photovoltaics

Jeffery A. Aguiar<sup>1\*</sup>, Sarah Wozny<sup>2</sup>, Nooraldeen R. Alkurd<sup>2</sup>, Terry G. Holesinger<sup>3</sup>, Toshihiro Aoki<sup>4</sup>, Maulik K. Patel<sup>5</sup>, Libor Kovarik<sup>6</sup>, Mengjin Yang<sup>1</sup>, Joseph J. Berry<sup>1</sup>, Mowafak. Al-Jassim<sup>1</sup>, Weilie Zhou<sup>2\*</sup>, and Kai Zhu<sup>1\*</sup>

<sup>1</sup> National Renewable Energy Laboratory, Golden, CO, 80401, USA

<sup>2</sup> Advanced Materials Research Institute, University of New Orleans, New Orleans, LA, 70148, USA

<sup>3</sup> Los Alamos National Laboratory, Los Alamos, NM, 80465, USA

<sup>4</sup> LeRoy Eyring Center for Solid State Science, Arizona State University, Tempe, AZ, 85287, USA

<sup>5</sup> Department of Materials Science and Engineering, University of Tennessee, Knoxville, TN, 37996, USA

<sup>6</sup> Environmental Molecular Sciences Laboratory, Pacific Northwest National Laboratory, P.O. Box 999, Richland, Washington 99352, USA

## **Abstract**

Organic-inorganic perovskites have emerged as an important class of next generation solar cells due to their remarkable low cost, band gap, and sub-900 nm absorption onset. Here, we show a series of *in situ* observations inside electron microscopes and X-ray diffractometers under device-relevant synthesis conditions focused on revealing the crystallization and growth process of the formamidinium lead-triiodide perovskite about the optimum temperature of 175° C. Direct *in situ* observations of the structure and chemistry over relevant spatial, temporal, and temperature scales enabled identification of key perovskite formation and degradation mechanisms related to grain evolution and interface chemistry. The lead composition was observed to fluctuate at grain boundaries, indicating mobile lead-containing species, a process found to be partially reversible about a key temperature of 175° C. Using low energy electron microscopy and valence electron energy loss spectroscopy, the lead is found to be bonded in the grain interior with iodine in a tetrahedral configuration. At the grain boundaries, the binding energy associated with lead is consequently shifted by nearly 2 eV and a doublet peak is resolved due presumably to a greater degree of hybridization and the potential for several different bonding configurations. At the grain boundaries there is adsorption of hydrogen and OH<sup>-</sup> ions, the result of residual water vapor trapped as a non-crystalline material trapped during formation. Insights into the relevant formation and decomposition reactions of formamidinium lead iodide at low to high temperatures, observed metastabilities, and relations to the photovoltaic performance were obtained and used to optimize device processing resulting in conversion efficiencies up to 17.09%.

## In Pursuit of Atomic-Scale Tomography

Thomas F. Kelly  
CAMECA Instruments, Inc.  
5500 Nobel Drive, Madison, WI USA 53711  
e-mail: thomas.kelly@ametec.com

There have been efforts of late to produce three-dimensional images at the atomic scale where every atom is accounted for and the position information is quite precise. All atoms in a two-dimensional thin film of boron nitride were imaged and identified by Krivanek et al. [1]. Scott et al. were able to produce three-dimensional images using electron tomography that show every atom in a gold nanoparticle containing over 7000 gold atoms [2]. Using atom probe tomography (APT), Moody et al. have shown three-dimensional images of several million atoms in an aluminum alloy where each atom is positioned correctly in a face-centered cubic lattice and 60% of the atoms are detected [3]. These are all impressive and important developments. They suggest what atomic-scale microscopy might ultimately achieve: recording with high precision the position and identity of every atom in a technologically relevant structure. This capability can fairly be termed atomic-scale tomography (AST).

If AST is to be achieved, it appears that APT and electron microscopy should be used synergistically to capture the strengths of one technique to overcome the limitations of the other. This question has been explored in detail [4] and the conclusion is that there are some ways that AST can be achieved. The instrumental developments needed to reach AST with APT as a basis include: trajectory corrections for precise atom placement and detecting 100% of the atoms without ambiguity in identity. The former may be achieved by imaging the specimen apex to enable precise ion trajectory simulation toward the detector. An electron column integrated into an atom probe can, in principle, record the specimen apex shape throughout an entire atom probe experiment. Detectors for recording all atoms might be based on superconducting materials [5]. If these detectors also record an ion's kinetic energy, then most time of flight-based ambiguities in peak identification can be eliminated [6].

This presentation will outline approaches that should be pursued to reach this end and review the current plans to build an atomic-scale tomograph.

- [1] O. L. Krivanek, et al., *Nat. Lett.*, vol. 464, p. 571, 2010.
- [2] M. C. Scott et al., *Nature*, vol. 483, pp. 444–447, 2012.
- [3] M. P. Moody et al., *Microsc Microanal.*, vol. 17, pp. 722–723, 2011.
- [4] T. F. Kelly et al., *Microsc. Microanal.*, vol. 19, pp. 652–664, 2013.
- [5] R. F. McDermott, J. R. Suttle, and T. F. Kelly, “Unpublished research,” 2015.
- [6] T. F. Kelly, *Microsc Microanal.*, vol. 17, pp. 1–14, 2011.

# **Atomic Force, Optical, and Super-Resolution Microscopy of DNA-Based Nanostructures**

Elton Graugnard

Micron School of Materials, Boise State University

DNA can be programmed into near-arbitrary macro-molecular structures by careful control of specific (Watson-Crick) and non-specific molecular interactions. Over the past decade, researchers have used the technique of "DNA Origami" to demonstrate the fabrication of a variety of two- and three-dimensional DNA nanostructures with structural features controlled at the single-nanometer scale ( $\sim 6$  nm). Such fine-scale structural control has generated interest in using DNA nanostructures for creating patterns in semiconductor memory manufacturing, which currently uses photolithography to create patterns with a resolution of  $\sim 20$  nm. At such resolutions, defect metrology has become increasingly time-intensive and difficult. This talk will describe research in to DNA origami patterning and the use of super-resolution microscopy for optical characterization and defect metrology.

## **Recording Optimal, Near-Atomic-Resolution Images of Cryogenic Specimens on a “Sub-Optimal” Transmission Electron Microscope**

David M. Belnap  
Departments of Biology and Biochemistry  
University of Utah  
Salt Lake City, Utah USA

The last few years have seen an explosion in the number of near-atomic-resolution structures determined by cryogenic transmission electron microscopy. This revolution has been facilitated by the invention of direct electron detectors that have greatly enhanced detective quantum efficiency. Currently, the best results are obtained on top-of-the-line TEMs, such as the FEI Titan Krios. These very expensive instruments are out-of-reach for many laboratories, which instead have access to very good, but "sub-optimal," TEMs. Examples of these instruments include the FEI Tecnai F20. Near-atomic resolution data can be obtained on these instruments by fine-tuning their operation.

## **A Force-Feedback High-Speed Atomic Force Microscope (HSAFM) and its Application to Biological Systems**

*Byung I. Kim*

Department of Physics, Boise State University  
1910 University Drive, Boise, Idaho

ByungKim@boisestate.edu

The recent advancement of high-speed atomic force microscopy (HSAFM) has enabled researchers to view the nanometer-scale dynamic behavior of individual biological and bio-relevant molecules at a molecular-level resolution under physiologically relevant time scales, which is the realization of a dream in the life sciences. These high-speed imaging applications now extend to the cellular/bacterial systems with the use of a smaller cantilever. Researchers viewed that the limitation originates from the size of the cantilever, as the cantilever response speed is proportional to the cantilever resonance frequencies. The use of a cantilever with high-resonant vibrational frequency allows more rapid vertical tip movement, thus obtaining high-speed imaging. The system has demonstrated image speeds up to one frame per second for small biomolecular structures such as DNA and one frame per ten seconds for larger biological systems such as bacteria. To understand many rapid large-scale biological phenomena, this imaging speed is not sufficient enough. Also, the use of smaller cantilevers creates some challenges, such as fabrication and signal detection with a smaller laser spot size.

Here we introduce an alternative approach to that of employing a small cantilever for high-speed imaging, called “force-feedback” HSAFM [1]. This new system utilizes our recent development of a cantilever-based optical interfacial microscope (COIFM) [2-5]. Rather than using a smaller cantilever, we still use a conventional-size self-actuation cantilever that is capable of fast response through the force-feedback mechanism. The force-feedback shortens the response time of the sensor, which is the most essential component for this HSAFM. We demonstrated that this force-feedback HSAFM is capable of acquiring large topographic images of *Escherichia coli* biofilms at approximately one frame per second in air. We discuss how the self-actuating cantilever and the piezo tube follow those larger biological topographic features during the HSAFM imaging process. This novel force-feedback HSAFM will contribute greatly to the studies of these large-scale biological phenomena through the improvement of the time resolution for scan sizes up to several micrometers. We also report the discovery of self-assembled chain-like water structures in a nanoscopic water meniscus confined between two oxidized silicon surfaces using this force-feedback technique [2,3]. Sawtooth-like oscillatory forces were observed when the two surfaces approached each other in the ambient environment.

### References:

- [1] B. I. Kim and R.D. Boehm, *Micron* **43**, 1372-1379 (2012)..
- [2] B. I. Kim., R. D. Boehm, J. R. Bonander, *J. Chem. Phys.* **139**, 054701 (2013).
- [3] B. I. Kim, J.A. Rasmussen, and E. J. Kim, *Appl. Phys. Lett.* **99**, 201902 (2011).
- [4] B. I. Kim, J. R. Bonander, and J. A. Rasmussen, *Rev. Sci. Instrum.* **82**, 053711 (2011).
- [5] J. R. Bonander and B. I. Kim, *Appl. Phys. Lett.* **92**, 103124 (2008)

## **Applications of computer programming in image acquisition, structural analysis, and machine vision**

Shixin Wang  
Micron Technology, Inc.

Today's powerful computer capability opens new territory in electron microscopy field. Computer based applications enable new technology, boost efficiency, increase data accuracy, and expand dimensions of human understanding. This presentation introduce several projects carried out in Micron TEM laboratory. They are: 1) Crystalline grain mapping based on diffraction scanning. This project utilizes automated microscopy control and image processing to reveal crystal orientation and dimension distribution. 2) Tableau DF imaging. This is a combination of microscope control and image analysis in TEM image mode, achieving high resolution crystal grain mapping efficiently. 3) Hybrid imaging. This is a multi-channel imaging utilizing EFTEM. Complimentary contrasts are recorded in a virtual multi-channel camera. This hybrid image is to bring out contrasts which are difficult to see in conventional imaging system. 4) EELS mapping with random scan. This is a computer controlled STEM and EELS collection with electron beam moves in a random fashion. The application of this technique is to reduce the effect of electron beam damage. 5) Feature extraction based on pattern recognition, showing the power of computer to analyze and finding complex features that are usually not easy to achieve with human brain. 6) TEM metrology utilizing computer vision to analyze the TEM/EFTEM/STEM images and to extract dimension information.

# Posters

# Characterization of Zirconium Oxides Using TEM and Automated Crystal Orientation Mapping Technique

Jatuporn Burns<sup>1,2</sup>, Patrick Price<sup>1</sup>, Darryl. P. Butt<sup>1,2</sup>, Isabella. J. van Rooyen<sup>3</sup>

<sup>1</sup>Department of Materials Science and Engineering, Boise State University, Boise, ID 83725

<sup>2</sup>Center for Advanced Energy Studies, Idaho Falls, ID 83401

<sup>3</sup>Fuel Design and Performance Department, Idaho National Laboratory, Idaho Falls, ID 83401, USA

## Abstract

The oxide-metal interface of the oxidized alloys were investigated in an effort to elucidate the connection between the oxide morphology and the oxidation behavior. The oxides formed on Zircaloy-3 and Zircaloy-4 alloys in air at temperatures 600 to 800 °C were characterized using transmission electron microscope (TEM) equipped with automated crystal orientation mapping system TOPSPIN. This technique allows nanoscale grains to be characterized in which conventional SEM-EBSD could not resolve. This study characterizes and compares the oxide morphology, structure, phase distribution, phase fraction of tetragonal to monoclinic, and intermetallic precipitates in both alloys. The oxides formed on zirconium alloys composed of monoclinic and meta-stable tetragonal phases and a layer of oxygen-rich zirconium. The oxide is mainly monoclinic phase with columnar and equiaxed grains.

## Open Access Materials Characterization Center

Josh Razink<sup>1</sup>, Robert Fischer<sup>1</sup>, Kurt Langworthy<sup>1</sup>

<sup>1</sup>Center for Advanced Materials Characterization in Oregon (CAMCOR)  
E-mail: [jrazink@uoregon.edu](mailto:jrazink@uoregon.edu), [robertf@uoregon.edu](mailto:robertf@uoregon.edu), [klangwor@uoregon.edu](mailto:klangwor@uoregon.edu)

The Center for Advanced Materials Characterization in Oregon (CAMCOR), located at the University of Oregon, houses more than \$30M in capital equipment available to industrial and academic researchers. CAMCOR's mission is to serve as an open-access “high-tech extension” service center by making its capital-intensive hardware and the technical expertise of its staff available to the external technical and scientific community as well as University of Oregon researchers. The facilities in CAMCOR are run by a team of experts who can provide expert advice, acquire and interpret complex data from cutting-edge materials, train users on the tools, teach courses/workshops on techniques, and offer consulting-style services. The facilities include: high-resolution transmission electron microscopy, focused ion beam microscopy, surface analysis (XPS/ToF-SIMS/Auger), NMR spectroscopy, electron microprobe analysis (EPMA), x-ray diffraction, and polymer characterization.

# Atomically-Resolved Chemical Mapping of a Model Oxide Interface: Challenges and Insights

Steven R. Spurgeon<sup>1</sup>, Yingge Du,<sup>1</sup> and Scott A. Chambers<sup>1</sup>

<sup>1</sup> Physical and Computational Sciences Directorate  
Pacific Northwest National Laboratory  
902 Battelle Blvd., Richland, WA 99352  
steven.spurgeon@pnnl.gov  
yingge.du@pnnl.gov  
sa.chambers@pnnl.gov

Small deviations in the chemistry or composition of nanoscale interfaces can give rise to significant changes in desirable emergent properties, such as ferroelectricity and magnetoelectricity, necessitating accurate probes of local structure to engineer such behavior. While aberration-corrected scanning transmission electron microscopy provides an excellent tool to probe nanoscale structure, the interpretation of atomically-resolved data is greatly complicated by complex beam-specimen interactions. In particular, it is unclear whether it is possible to directly interpret chemical maps of unknown structures without substantial prior knowledge.

Here we describe our analysis of a model oxide interface using a combination of aberration-corrected high-angle annular dark field (STEM-HAADF), electron energy loss spectroscopy (STEM-EELS), and energy-dispersive X-ray spectroscopy (STEM-EDS). We describe the challenges involved in the quantification of atomic maps, showing that estimates of interfacial mixing can vary widely depending on the technique used. We consider our results in light of multislice simulations, which allow us to systematically probe the effect of thickness on the delocalization of the resulting chemical maps. Our calculations show that even in the case of on-axis imaging of reasonably thin and atomically abrupt interfaces, delocalization of ionization signals can give rise to an artificially broadened interface structure. From these results we describe the limitations of each method and suggest potential ways to facilitate the interpretation of atomic maps. Our study cautions against the direct measurement of interfaces using any single technique and emphasizes the need for a correlative approach to nanoscale materials characterization.

## IMAGING DYNAMIC PROCESSES IN LIQUIDS: APPLICATIONS FOR BATTERIES

B Layla Mehdi<sup>1,2</sup>, Andrew Stevens<sup>3</sup>, Chiwoo Park<sup>5</sup>, Karl T Mueller<sup>1,2,6</sup>, Nigel D. Browning<sup>1,4</sup>,

<sup>1</sup>Joint Center for Energy Storage Research (JCESR), Pacific Northwest National Laboratory (PNNL), Richland, WA 99352, USA

<sup>2</sup>Physical and Computational Science Directorate, PNNL, Richland, WA 99352, USA

<sup>3</sup>National Security Directorate, PNNL, Richland, WA 99352, USA

<sup>4</sup>Materials Science and Engineering, University of Washington, Seattle, WA 98195, USA

<sup>5</sup>Industrial & Manufacturing Engineering, Florida State University, Tallahassee, FL 32306, USA

<sup>6</sup>Department of Chemistry, Penn State University, University Park, PA, 16802, USA

Lithium (Li)-ion batteries are currently used for a wide variety of portable electronic devices, electric vehicles and renewable energy applications. However, the practical application of Li metal anode systems has been highly problematic. The main challenges involve controlling the formation of a solid-electrolyte interphase (SEI) layer and the suppression of Li dendrite growth during the charge/discharge process (achieving “dendrite-free” cycling). The SEI layer formation continuously consumes the electrolyte components creating highly resistive layer, which leads to the rapid decrease of cycling performance and degradation of the Li anode. The growth of Li dendrites at the anode contributes to rapid capacity fading and, in the case of continuous growth, leads to internal short circuits and extreme safety issues.

Here, we demonstrate the application of an *operando* electrochemical cell to study dynamic processes at the electrode/electrolyte interface and investigate the role and mechanism of electrolyte additives during Li deposition/stripping in Li-ion battery. We use two electrolytes, LiPF<sub>6</sub> in propylene carbonate (PC) with different trace-amounts of water (10 and 50 ppm). Figure 1A shows a comparison of the cyclic voltammograms for the two electrolytes and Figure 1B shows the corresponding amount of Li deposited/stripped during these cycles (Figure 1C and D shows representative STEM images of the process). The higher concentration of water, leads to an increased concentration of highly conducting LiF in the SEI layer, leading to a larger grain size through increased diffusion of Li ions during battery cycling. SEM images show Li deposited on a Cu electrode surface in the presence of 10 ppm (Figure 2E) and 50 ppm (Figure 1F) of water at a current density of 1mA/cm<sup>2</sup> for 15 h. The Li deposits in the electrolyte containing 10 ppm shows a typical dendritic microstructure. However, the electrolyte with 50 ppm of water forms smooth, thin and dense dendritic layer. This result provides crucial insights into the performance of Li metal anodes and their successful incorporation into the next generation battery system.

**Acknowledgments** This research is part of the Chemical Imaging LDRD Initiative at PNNL, a multi-program laboratory operated by Battelle for the U.S. DOE under Contract DE-AC05-76RL01830. This work was partially supported by JCESR, an Energy Innovation Hub funded by DOE-BES. A portion of the research was performed using EMSL, a national scientific user facility sponsored by DOE-BER and located at PNNL. C.P. acknowledges support from the FSU COFRS Award 032968, the Ralph E. Powe Junior Faculty Enhancement Award, and NSF-CMMI-1334012.

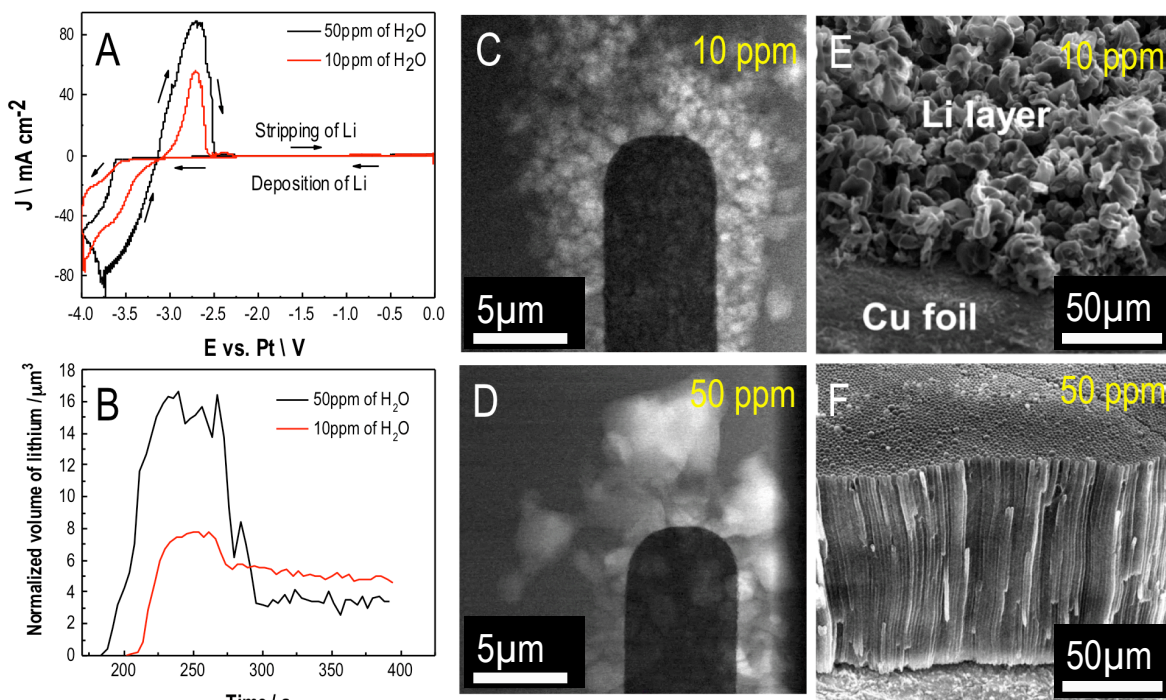


**Figure 1.** Cyclic voltammograms of the  $\text{LiPF}_6/\text{PC}$  electrolyte with 10 ppm (red) and 50 ppm (black) of water (A) and quantified total area of Li deposited and stripped for the electrolyte with 10 ppm (red) and 50 ppm (black) of water. BF STEM images of Li deposits/grains at the interface between the Pt working electrode in the presence of 10 ppm (C) and 50 ppm (D) of water and corresponding SEM images of Li deposited at the Cu foil after 15h with a  $1\text{mA}/\text{cm}^2$  current density for 10 ppm (E) and 50 ppm (F).

## Peculiar Protrusions: Examining the Chemistry of the eighteenth century Oil-on-Copper Paintings using Microscopy and Spectroscopy

Robin A. McCown<sup>a</sup>, Bogdan Makar<sup>a</sup>, Sierra Ludwig<sup>a</sup>, Mari Carmen Casas-Pérez<sup>b</sup>, Glenn Gates<sup>c</sup>, Darryl P. Butt<sup>a</sup>

<sup>a</sup> Boise State University, Materials Science Department

<sup>b</sup> DICIM Universidad Autónoma de San Luis Potosi

<sup>c</sup> Walters Art Museum

Oil on copper has been a common art form for several hundred years due to its beauty, ease of use, and widespread availability. Many of such paintings are still remarkably preserved, but exceptions exist. This work focuses on a painting titled *The Expulsion of Hagar* (1767), one of the several oil on copper painted by C.W. Dietrich. Small protrusions and eruptions (~1mm) were identified on the painting surface, disrupting the layers of primer, paint and varnish that Dietrich originally applied. Optical microscopy, SEM, and TEM, coupled with EDS and Raman spectroscopy, have been used to characterize paint chips from both degraded and non-degraded areas of this painting. Upon further analysis, this team determined that a chemical reaction between the copper metal, an organic layer and the lead-based inorganic primer could be the cause of degradation. This data, combined with knowledge of copper-processing practices, yields a result that may have implications for other oil-on-copper paintings showing similar time-based damage. The presence of Cu<sub>2</sub>O is confirmed via TEM-EDS and electron diffraction, indicating corrosion likely occurred. Preliminary results suggest a process involving copper soap and nickel arsenide.

### Contact Information:

Robin A. McCown: [robinmccown@boisestate.edu](mailto:robinmccown@boisestate.edu), 208-447-7055

Bogdan Makar: [danniemakar@u.boisestate.edu](mailto:danniemakar@u.boisestate.edu), 208-914-8608

Sierra Ludwig: [sierraludwig@boisestat.edu](mailto:sierraludwig@boisestat.edu), 808-359-4268

Mari Carmen Casas-Pérez: [casas.maricarmen@gmail.com](mailto:casas.maricarmen@gmail.com), 208-576-6112

Glenn Gates: [ggates@thewalters.org](mailto:ggates@thewalters.org), 410-547-9000, ext 365

Darryl P. Butt: [darrylbutt@boisestate.edu](mailto:darrylbutt@boisestate.edu), 208-426-1054

# An atomic mechanistic picture of ethane oxidation over M1 MoVTeNb oxide: the promoter role of Te

Yuanyuan Zhu<sup>1</sup>, Eric Jensen<sup>1</sup>, Peter V. Sushko<sup>1</sup>, Libor Kovarik<sup>2</sup>, Daniel Melzer<sup>3</sup>, Maricruz Sanchez-Sanchez<sup>3</sup>, Johannes A. Lercher<sup>3</sup> and Nigel D. Browning<sup>1,4</sup>

<sup>1</sup> Physical & Computational Sciences Directorate, Pacific Northwest National Laboratory, Richland, WA 99352, USA

<sup>2</sup> Environmental Molecular Sciences Laboratory and Institute for Integrated Catalysis, Pacific Northwest National Laboratory, Richland, WA 99352, USA

<sup>3</sup> Department of Chemistry and Catalysis Research Center, Technical University of Munich, Garching 85748, Germany

<sup>4</sup> Department of Materials Science and Engineering, University of Washington, Seattle, WA 98195, USA

M1 phase of mixed MoVTeNb oxide is, by far, the most promising ethane oxidative dehydrogenation (ODH) catalyst towards industrialization. However, an independent and valid reaction mechanism for ethane ODH over M1 has not been established to date. To provide sound postulations for ethane oxidation mechanism, it is essential to develop our understanding on the atomic mechanistic of the MoVTeNb oxide, especially at its active site. Active sites facilitate reactant/product molecules absorption/desorption, bond rearrangement and electron exchange, but active sites often undergo themselves geometric and electronic structural changes under working conditions. In ODH of alkanes, understanding the catalytically relevant sites in M1 MoVNbTe oxide remains as one of the greatest challenges [1, 2]. Among various structural characterization tools, environmental ADF-STEM offers unique directly interpretable incoherent imaging of potential catalytic sites at the atomic level [3, 4]. In this work, we demonstrate systematic ESTEM analysis of the atomic configuration of the M1 (001) basal plane, where active sites are proposed to be located, after quenching from the ethane ODH operation temperature of 400 °C in the presence of various gas feeds.

Fig. 1 summarizes the structural evolution of the same M1 (001) at various heating durations under each carefully chosen atmospheric conditions. Here, we employed a dedicated field-emission ETEM (FEI Titan 80-300), equipped with differential pumping system allowing controlled gas pressure around the sample. To alleviate heating-introduced sample drifting and off-zone, we adopted a slow-heating-and-fast-quenching protocol that preserves the development of M1 structure at different reaction stages for atomic STEM observation. To achieve a sound sampling statistics, we developed an automated line profile analysis capable of robustly locating over 200 structure units (marked by diamonds) with effective background subtraction and atomic displacement calculation for each STEM image. This in-depth analysis reveals unexpected structural modifications of atomic sites round the cation site S2 in the M1 (001) plane when exposed to different gas feeds at different heating duration. Combining STEM image quantification and simulation as well as *ab initio* (density functional theory) simulations of the temperature-induced transformations of the atomic structure and associated electronic structure changes, we propose a new activation mechanism for the M1 active sites under working conditions for ethane oxidation as well as for the evolution of such active sites from the room-temperature stable catalyst precursor.

References:

- [1] R Schlögl, Topics in Catalysis 54 (2011) 627.  
 [2] C Gaertner, A van Veen and J Lercher Chemcatchem 5(2013) 3196.  
 [3] E Boyes and P Gai, Comptes Rendus Physique 15 (2014) 200.  
 [4] N Browning *et al*, Chemcatchem 5(2013) 2673.  
 [5] This research is part of the Chemical Imaging Initiative conducted under the Laboratory Directed Research and Development Program at Pacific Northwest National Laboratory (PNNL). PNNL, a multiprogram national laboratory, is operated by Battelle for the Department of Energy under Contract DE-AC05-76RLO1830.

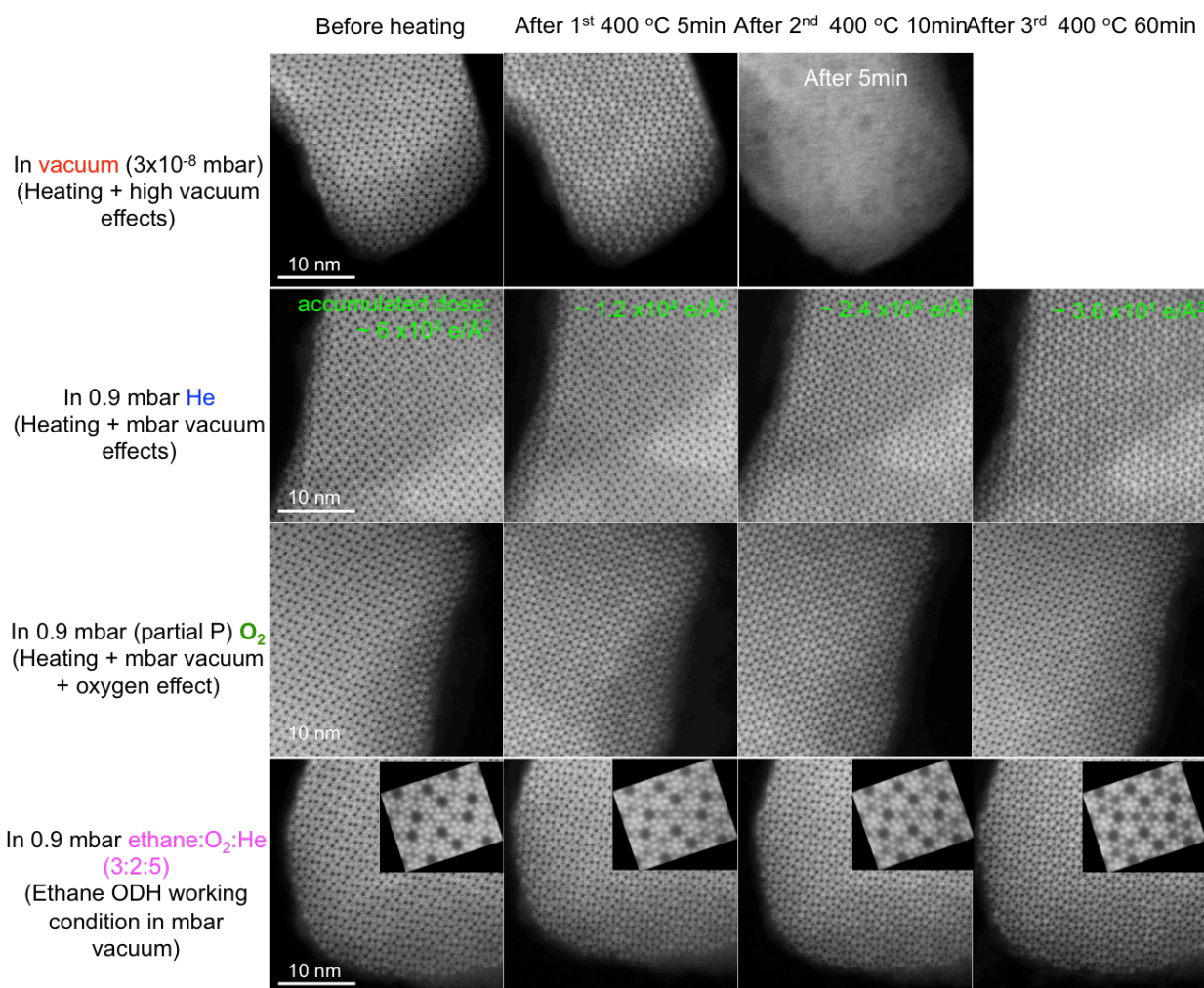


**Figure 1.** Atomic resolution ADF-STEM snapshots of M1 (001) planes before and after thermally treated for different heating durations in four systematically selected atmospheric conditions. The inserts in the 4<sup>th</sup> row are averaged STEM images showing the structural evolution of M1 under ethane oxidation condition.

## Fast and simplified Lorentz TEM for use on uniform thickness magnetic samples

**Jordan Chess:** Department of Physics, 1274 University of Oregon, Eugene OR 97403-1274; jchess@uoregon.edu

**Sergio Montoya:** Center for Magnetic Recording Research, University of California San Diego, 9500 Gilman Dr, La Jolla, CA 92093; samontoy@ucsd.edu

**Tyler Harvey:** Department of Physics, 1274 University of Oregon, Eugene OR 97403-1274; trh@uoregon.edu

**Eric Fullerton:** Center for Magnetic Recording Research, University of California San Diego, 9500 Gilman Dr, La Jolla, CA 92093; efullerton@ucsd.edu

**Ben McMorran:** Department of Physics, 1274 University of Oregon, Eugene OR 97403-1274; mcmorran@uoregon.edu

Lorentz transmission electron microscopy (LTEM) is one of a very few techniques for providing direct images of magnetic features at the nanoscale, and it has played an important role in advancing both our fundamental understanding of and technological applications for magnetic materials<sup>1</sup>. For Fresnel-contrast LTEM the transport of intensity equation (TIE), is the tool of choice for exit wave phase retrieval and quantitative determination of the local magnetic induction through the sample thickness<sup>2</sup>. Recently the combination of TIE and LTEM have helped researchers advance our understanding of the emerging field of magnetic skyrmions<sup>3-5</sup>. A magnetic skyrmion is a topologically non-trivial magnetization texture that has attracted the attention of the magnetics community due in large part to the potential application as information carriers in low-power memory applications including racetrack memory. Here we propose a simplified TIE approach that is applicable to many skyrmionic materials as well as many other technologically relevant magnetic samples. Similar to the work by Paganin et al. and Eastwood et al. in which they showed that a thickness map of a homogeneous material could be determined from a single defocused image<sup>6,7</sup>: here we show that for a uniform thickness magnetic film the magnetic portion of the electron phase shift can be determined from a single defocused image. With this approach the magnetic portion of the phase is determined by solving the equation,

$$\nabla_{\perp}^2 \phi_m = -\frac{2\pi}{\lambda \Delta f} \left( 1 - \frac{I(r_{\perp}, \Delta f)}{I_0} \right).$$

An advantage of this phase retrieval method beyond the immediate reduction in experimental difficulty is the possibility to determine the local magnetic induction during a time-dependent measurement such as during a magnetic field sweep or a current pulse. This opens a possibility of observing magnetic evolution at fast timescales using 4D-TEM. To investigate the regime of applicability for this technique we applied it to both simulated (see FIG.1) and experimental (see FIG.2) data.

1. Marc De Graef & Yimei Zhu. *Magnetic Imaging and Its Applications to Materials, Volume 36*. (San Diego : Academic Press, 2001).
2. Kohn, A., Habibi, A. & Mayo, M. *Ultramicroscopy* **160**, 44–56 (2016).
3. Morikawa, D. *et al. Appl. Phys. Lett.* **107**, 212401 (2015).
4. Tokunaga, Y. *et al.* A new class of chiral materials hosting magnetic skyrmions beyond room temperature. *Nat. Commun.* **6**, 7638 (2015).
5. Mochizuki, M. *et al. Nat. Mater.* **13**, 241–246 (2014).
6. Paganin, D., Mayo, S. C., Gureyev, T. E., Miller, P. R. & Wilkins, S. W. *J. Microsc.* **206**, 33–40 (2002).
7. Eastwood, S. A., Paganin, D. M. & Liu, A. C. Y. *Opt. Lett.* **36**, 1878 (2011).

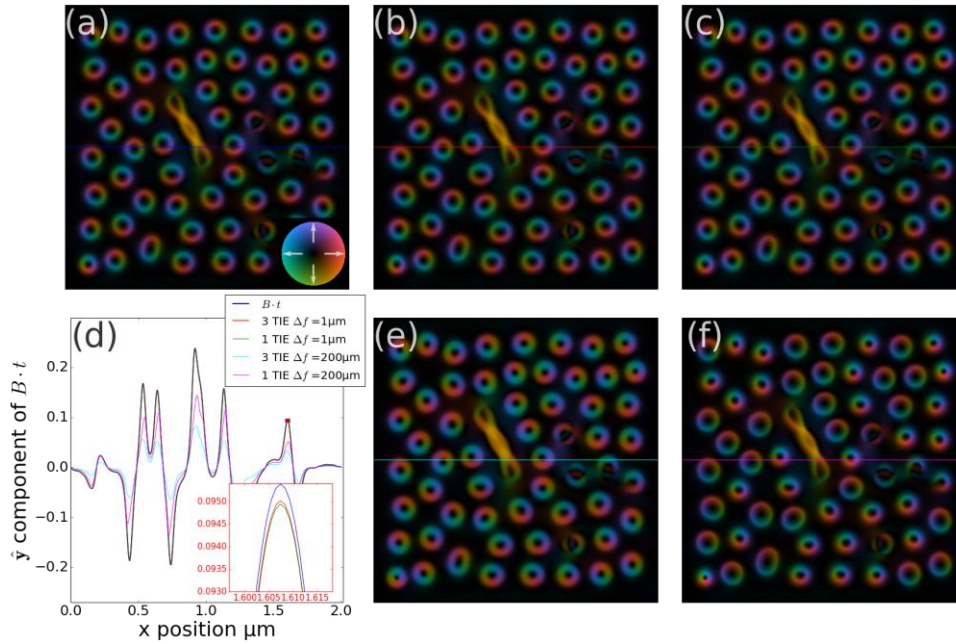


**Figure 1.** Panel (a) local magnetic induction results of FastMag micromagnetic simulation hue/saturation indicates direction of magnetic field direction/strength; (b), (c) standard 3 image TIE and single image TIE 1  $\mu\text{m}$  obtained from numerically calculated focal series; (d) y-component of the magnetic induction through the lines in the color images; (e), (f) 200  $\mu\text{m}$  standard 3 image TIE and single image TIE obtained from numerically calculated focal series.

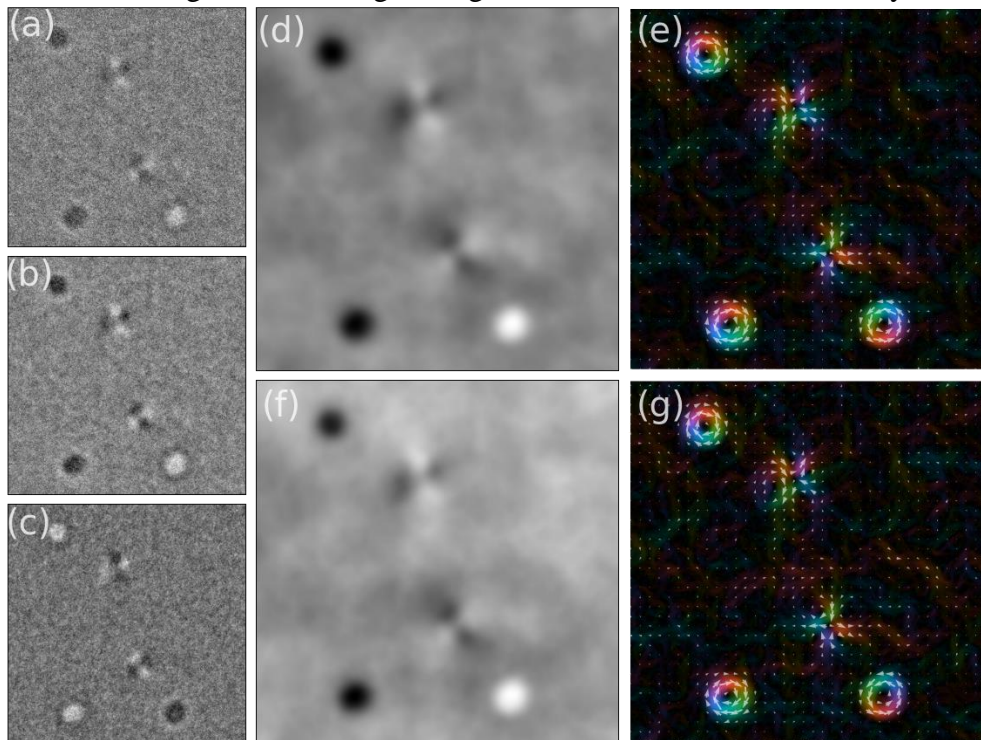


**Figure 2.** Panel (a), (c) experimental underfocused/overfocused Fresnel-contrast image of Fe:Gd thin film; (b) approximate z derivative of image intensity used for standard TIE; (d) phase calculated using standard TIE; (f) phase calculated using only image (a); (e), (g), magnetic induction calculated from phase on left.

# X-ray fluorescence elemental imaging, and micro analysis of plant tissue samples

Ursula E.A. Fittschen<sup>1</sup>, Ricarda Hoehner<sup>2</sup>, Hans-Henning Kunz<sup>2</sup>

<sup>1</sup>Chemistry Department, Washington State University, Pullman 99164-4630,

[Ursula.fittschen@wsu.edu](mailto:Ursula.fittschen@wsu.edu),

<sup>2</sup>School of Biological Sciences Washington State University, Pullman 99164-4630,

Micro X-ray fluorescence (MXRF) allows for spatial resolved elemental analysis and imaging of condensed matter. X-ray probes in general offer high penetration depth and therefore allow for 3D observations of multi-phase systems e.g. living organisms. Whereas modern synchrotron sources easily offer spot sizes of around 100-500 nm, laboratory-based instruments have focal spots in the mesoscopic range 10-30  $\mu\text{m}$  focal diameter size. The resolution of Micro-X-ray fluorescence is sufficient to make it a powerful tool in quantitatively visualizing changes in elemental distribution on the microscale caused by plant development effects or by loss or gain-of-function mutations in the plant genome. This presents a powerful tool to understand complex physiological processes in context such as the link between the plant ion homeostasis and photosynthetic efficiency.

Recently, we finished the design and assembly of our first laboratory-based X-ray microscope at WSU. Here, we will present our first results obtained on several plant samples from the model plant *Arabidopsis thaliana*. Our preliminary data provide insights regarding the spatial ion distribution in plants and provide high data resolution which represents a fundamental requirement for all the fine-tuned biochemical processes occurring in different plant tissues simultaneously. In the near future we expect to have additional in depth capabilities with spatial resolution of ca.  $20 \times 20 \times 20 \mu\text{m}^3$  to be available.

# Controlled Dose for *in situ* (Scanning) Transmission Electron Microscopy Observations of Iron Oxide Nanoparticle Dynamics

Ryan Hufschmid,<sup>1</sup> Eric Teeman,<sup>1</sup> B. Layla Mehdi,<sup>2</sup> Eric Jensen,<sup>2</sup> Kannan M. Krishnan,<sup>1</sup> and Nigel D. Browning<sup>1,2</sup>

<sup>1</sup> Department of Materials Science and Engineering, University of Washington, Box 352120, Seattle, WA 98195-2129, USA

<sup>2</sup> Fundamental and Computational Sciences Directorate, Pacific Northwest National Laboratory, PO Box 999, Richland, WA 99352, USA

Recent developments in *in situ* liquid cell Transmission Electron Microscopy (TEM) techniques enable direct investigation of nano-systems in relevant environments. By encapsulating liquid between two electron transparent silicon nitride membranes the sample can be introduced into the TEM column without compromising vacuum. This allows for dynamic nanoscale phenomena to be directly observed *in situ* at high spatial and temporal resolution under controlled electron dose conditions allowing for imaging and chemical analysis.

In this work we observe magnetite (Fe<sub>3</sub>O<sub>4</sub>) nanoparticles and alter surface chemistry to systematically study their behavior and the effects of the electron beam *in situ*. Iron oxides are ubiquitous in natural systems, from biomineralization to the terrestrial carbon cycle, and serve as a platform for a range of engineered applications, for example, Magnetic Particle Imaging (MPI). Interactions between iron oxides, solvents, minerals, small molecules, and tissues are fundamental to these diverse systems. Magnetite nanoparticles are synthesized by thermal decomposition of Fe<sup>3+</sup> oleate, and are single crystalline, monodisperse, and phase-pure to ensure uniform physio-chemical and magnetic properties. As-synthesized particles are terminated with oleic acid and soluble in organic solvents, and are transferred to aqueous phase by coating with an amphiphilic co-polymer then functionalized with positive and negative charged species.

Here we demonstrate application of the *in situ* liquid (S)TEM cell to study behavior of magnetite nanoparticles with different surface chemistries in organic and aqueous solutions. We show that magnetite in the presence of organic solvent (1-octadecene) is stable up to relatively large electron beam doses (>50 e-/Å<sup>2</sup>s). However, nanoparticles undergo a dissolution process in the presence of water and resulting radiolysis byproducts, even under relatively low dose conditions of <1 e-/Å<sup>2</sup>s. The dissolution process can be tuned, as it is proportional to the e-beam dose delivered to the sample during the experiment, and dependent on surface chemistry of the functionalized magnetite nanoparticles. We show that nanoparticles with charged functional groups interact with reactive species in solution, accumulating ions at the particle surface, slowing dissolution, and enhancing particle interaction and agglomeration. We discuss how to mitigate and utilize the reductive effects of the electron beam, both in the case of magnetite and more broadly for other iron oxide/hydroxide phases, beam sensitive oxide materials, and in general for *in situ* TEM experiments.

*This work was funded by the Laboratory Directed Research and Development program at Pacific Northwest National Laboratory (PNNL). This work was performed in part using the William R. Wiley Environmental Molecular Sciences Laboratory, a US Department of Energy (DOE) national scientific user facility sponsored by the DOE's Office of Biological and Environmental Research and located and PNNL. PNNL is operated by Battelle for DOE under Contract DE-AC05-76RL01830. This work was also supported by NIH 1R01EB013689-01/NIBIB, 1R41EB013520-01, 1R42EB013520-01.*

## Compressive Reconstruction for STEM Imaging of *In-Situ* Processes

Thomas Warfel, Andrew Stevens, Elizabeth Jurrus, Layla Mehdi,  
Dimitri Zarzhitsky, Nigel Browning, Mark Greaves  
Pacific Northwest National Laboratory, Richland, WA

Sample damage caused from the imaging electron beam limits the use of high-resolution scanning transmission electron microscopy (STEM), especially for in-situ experiments. The goal of this work is to reduce the specimen exposure to beam current while maintaining image quality and resolution.

We address this problem by acquiring “sparse images” from the electron microscope, followed by computer reconstruction to inpaint missing data and minimize overall noise. We acquire “sparse images” by measuring a (randomly-distributed) fraction of the desired image pixels and by reducing the beam current per pixel (more noise per pixel). Our final images are reconstructed from the acquired samples using a constrained pattern-matching algorithm coupled with a machine-learned “patch dictionary.” The pattern-matching algorithm fits the acquired samples as a weighted sum of overlapped dictionary patches and is constrained to minimize both the number of patches used as well as the residual error<sup>1</sup>. This method results in high resolution images reconstructed with a low error rate while also reducing the sample’s electron beam exposure.

While the results of this method are promising, the time required to reconstruct the image after acquisition has been a major bottleneck. The Analysis in Motion (AIM) Initiative at PNNL has made efforts to improve this process through progressive analysis and refactoring of prototype code and migration to a high performance computing platform. Our approach attempts to improve the running time through i) parallelizing large portions of the algorithm that can run as independent processes, ii) dividing the image into overlapping sub images that can be solved independently, iii) reducing the numerical precision for portions of the method, and iv) reusing existing dictionaries. For future work we plan to deploy an MPI-capable version across an HPC environment, further enabling a real time approach for image acquisition and reconstruction.

---

<sup>1</sup> Mingyuan Zhou, Haojun Chen, John Paisley, Lu Ren, Guillermo Sapiro and Lawrence Carin, "Non-Parametric Bayesian dictionary learning for sparse image representations," Neural Information Processing Systems (NIPS), 2009

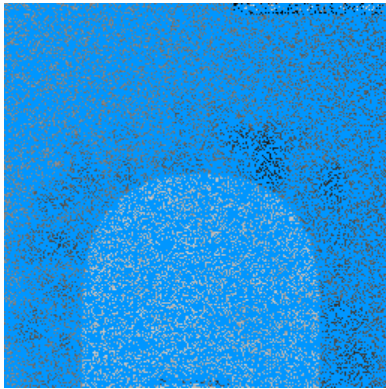


**Figure 1 - Example STEM image randomly missing 75% of pixels**

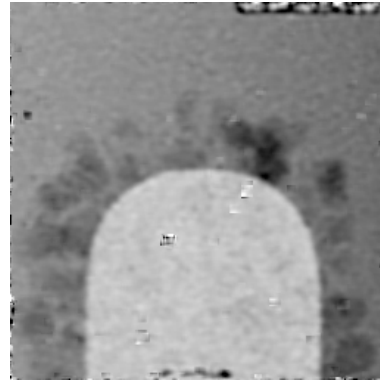


**Figure 4 - Same reconstruction at 500 iterations**

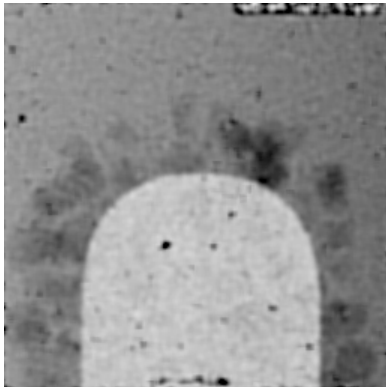


**Figure 2 - Reconstruction starting from precalculated patch directory, at 20 iterations**

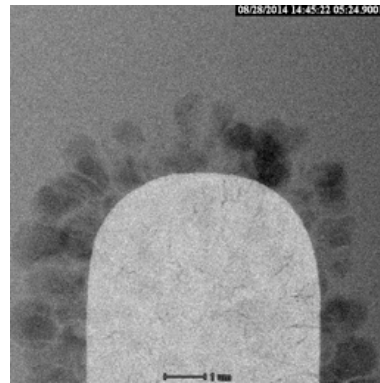


**Figure 5 - "Ground truth" for our undersampled image**

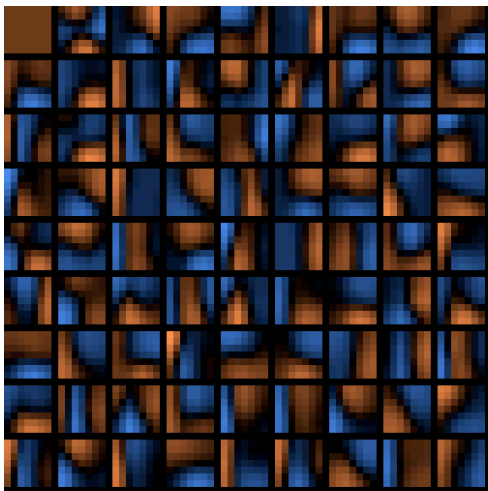


**Figure 1 - Starting (previously calculated) patch dictionary. Orange represents positive values, blue represents negative values.**

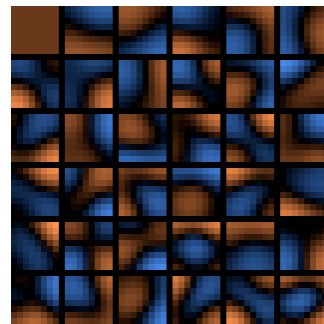


**Figure 2 - Final patch dictionary that evolved to reconstruct image**